Tetraazaoctaphyrin — A biimidazole-containing expanded porphyrin[1]

Jonathan L. Sessler, Bobbi L. Rubin, Marcin Stępień, Thomas Köhler, G. Dan Pantos, and Vladimir Roznyatovskiy

Abstract: A series of expanded porphyrins, incorporating biimidazoles and bipyrroles within their macrocyclic framework, has been synthesized. Insights into the complex conformational characteristics of these systems were obtained from two-dimensional NMR spectroscopic studies. The relative energy values for the various asymmetric structures inferred from these analyses were compared using DFT molecular modeling calculations.

Key words: macrocycles, expanded porphyrins, imidazoles, pyrroles, biimidazoles, supramolecular chemistry, heterocycles.

Résumé : On a réalisé la synthèse d'une série de porphyrines agrandies qui incorporent des biimidazoles et des bipyrroles dans le squelette de leur macrocycle. Sur les bases des études de spectroscopie RMN bidimensionnelle, on a extrait des donnés qui permettent de mieux comprendre les caractéristiques conformationnelles complexes de ces systèmes. On a comparé les valeurs relatives d'énergie de diverses structures asymétriques déduites de ces analyses à celles obtenues par des calculs de modélisation moléculaire sur la base de la théorie de la fonctionnelle de densité.

Mots clés : macrocycles, porphyrines agrandies, imidazoles, pyrroles, biimidazoles chimie macromoléculaire, hétérocycles.

[Traduit par la Rédaction]

Introduction

A new subdiscipline of porphyrin chemistry, involving the synthesis and study of large oligopyrrole macrocycles, so-called expanded porphyrins, was instigated by the serendipitous discovery of sapphyrin by Woodward and co-workers in the mid 1960s (1). In the decades since that time, the field of expanded porphyrin chemistry has grown into a large and vibrant subfield of macrocyclic chemistry (2). Expanded porphyrins have been studied in the context of molecular recognition with anionic, cationic, and neutral substrates (3). Part of what is driving this research is the promise that these systems show in various practical applications, ranging from drug development to anion recognition (4–7). Work in this area has also been inspired by less prosaic motivations, including the synthetic challenge of constructing new oligopyrrolic macrocycles and their inherent aesthetic appeal.

Received 11 October 2005. Accepted 30 November 2005. Published on the NRC Research Press Web site at http://canjchem.nrc.ca on 8 June 2006.

J.L. Sessler,[2] B.L. Rubin, M. Stępień, T. Köhler, G.D. Pantos, and V. Roznyatovskiy.[3] Department of Chemistry and Biochemistry, The University of Texas at Austin, 1 University Station A5300, Austin, TX 78712-0165, USA.

[1]This article is part of a Special Issue dedicated to Dr. Alfred Bader.

[2]Corresponding author (e-mail: sessler@mail.utexas.edu).
[3]Present address: Department of Chemistry, M.V. Lomonosov Moscow State University, Leninskie Gory, 119899 Moscow, Russian Federation.

[4]J.L. Sessler and J.T. Lee. Unpublished results.

Most known expanded porphyrins, with the exception of Schiff-base macrocycles, have been constructed from pyrrole and its closely related heterocyclic analogues, furan, thiophene, and selenophene. Recently, efforts have shifted towards incorporating imidazoles and biimidazoles into porphyrin-like structures. Youngs et al. (8) reported the synthesis of a series of cyclophane complexes, or porphyrinoids, which contained imidazoliums incorporated into the skeletal framework of the macrocycle. In 2003, the research groups of Allen (9) and Nonell (10) separately reported the first biimidazole-based porphycene analog, imidacene. There have also been a number of reports that describe the incorporation of imidazole or imidazolium cations into other macrocyclic structures (11–14). These systems show great promise in both anionic and cationic recognition and are made especially interesting because they are potentially capable of recognition both inside and outside the skeletal framework. In spite of this promise, biimidazoles, as opposed to imidazoles, have yet to be incorporated into expanded porphyrin-type frameworks. We report here the first example of such a system, namely 3,6,21,24-tetraaza[32]octaphyrin(1.0.1.0.1.0.1.0).

Results and discussion

The synthesis of tetraazaoctaphyrin target **3** was carried out in a single step via the condensation of biimidazole **1** with bis-α-free bipyrrole **2** under dilute conditions (Scheme 1). Biimidazole **1a** was prepared according to the literature and **1b** was synthesized using an extension of this same basic methodology (10). Bipyrroles **2a**–**2c** were synthesized according to the literature (15, 16).[4] The condensation of biimidazole **1** with bipyrrole **2** was performed in a

 doi:10.1139/V06-068

methanol–tetrahydrofuran (THF) mixture using trifluoroacetic acid (TFA) as the acid catalyst. After column chromatographic work-up over silica gel, tetraazaoctaphyrins **3a**–**3e** were obtained in yields ranging from 26% to 69%, depending on the substrates used. The compounds obtained in this way are unstable when exposed to oxygen and decompose over time. Thus, they were stored in a freezer under a blanket of argon. Under these conditions, little decomposition was seen for a period of 1 week. Elemental analysis was used as a means of characterization and repeatedly resulted in total carbon, hydrogen, and nitrogen counts of 95%–96% of the theoretical values. XPS analysis revealed the presence of silicon and oxygen, which is supported by a singlet near 0 ppm observed in the ^{1}H NMR spectra of **3a**–**3e**, attributable to a dimethyl siloxane compound. Efforts to remove the impurity included recrystallization, trituration, and extraction, but unfortunately all proved unsuccesful. If, however, the carbon, hydrogen, and nitrogen percentage is normalized to 100% and compared with a theoretical percentage of the same elements, thus accounting for the amount of impurity in these percentages, the experimental results fall within acceptable error values (i.e., $\Delta < 0.20\%$). In an additional experiment, the solvent was passed through a blank column under identical conditions and the siloxane was identified in the eluate by XPS and ^{1}H NMR spectroscopy, thus establishing the silica gel as the likely source of the impurity.

The UV–vis absorption spectrum of **3b**, the prototypical tetraazaoctaphyrin chosen for detailed study, is characterized by a Soret-type band at 299 nm and a Q-type band at 633 nm (Fig. 1). These features, particularly the latter long-wavelength absorption band, are considered diagnostic of an extended conjugated system (17). Dilute solutions of tetraazaoctaphyrin **3** in methylene chloride are blue and fluoresce red (Fig. 2). For the fluorescence emission experiments, excitation was performed at 578 nm, while the emission maximum was observed at 670 nm.

The one-dimensional ^{1}H NMR spectrum of **3b** recorded in dichloromethane-d_2 is shown in Fig. 3. It is apparent from an inspection of this spectrum that the solution structure of **3b** does not exhibit the fourfold symmetry implied by the representation of the macrocycle given in Scheme 1. The actual conformation has only twofold symmetry, which can be inferred from the doubled number of peaks in the aromatic and alkyl regions. The signal at 9.87 ppm integrates to two protons and most likely corresponds to a pyrrole NH proton. When studied as a solution in DMSO-d_6, an additional peak with the same integral intensity can be observed at 10.8 ppm. In dichloromethane-d_2, this signal is broadened by exchange and cannot be observed. Such a solvent dependence is typically found for imidazole NH protons. Based on these findings, the signal is assigned as an imidazole NH; however, its exact placement on the biimidazole unit could not be determined. Chemical shifts of the NH and meso protons indicate an absence of overall macrocyclic aromaticity.

The doubled spectral pattern, indicative of symmetry lowering, is also seen for the other tetraazaoctaphyrin derivatives. It should, however, be noted that the doubled signals assigned to the dominant species present in solution are often accompanied by ones ascribable to an impurity, which gives rise to a single set of peaks. The admixture inferred on this basis cannot be separated by chromatography (all samples yield a single peak on the HPLC chromatogram). While the identity of the additional species could not be ascertained, it is thought that it may correspond to a different symmetrical conformation for each of the different derivatives of **3**.

Fig. 1. Absorbance (—) and fluorescence spectra (----) of **3b** in CH_2Cl_2.

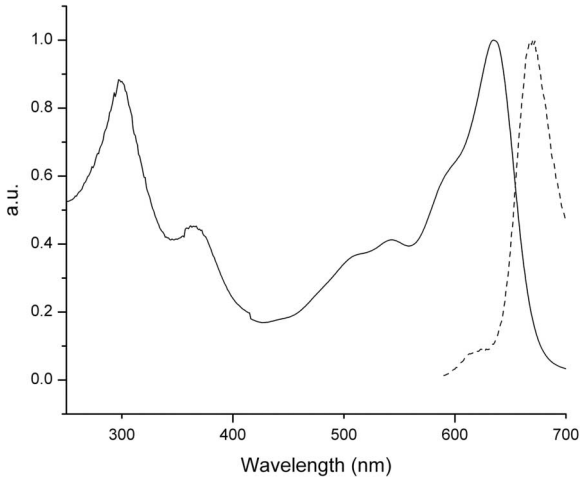

Fig. 2. Dilute solution tetraazaoctaphyrin **3b** in methylene chloride in the absence (left) and presence (right) of an illuminating black light (365 nm).

The assignment of the signals presented in Fig. 3 follows the labeling pattern given in Scheme 2. These assignments were deduced using two-dimensional NMR spectroscopy (COSY and ROESY maps). Figure 4 shows representative expansions of the COSY spectrum, used to establish connectivity within the aryl rings and alkyl chains. There is a significant crowding of signals in the alkyl region, which was resolved on the COSY map. Further insight into the structure and conformation of **3b** was gained from an analysis of the ROESY spectrum (Fig. 5).

Based on selected ROE cross-peaks, it was possible to assign unequivocally each of the signals to one of the two

Scheme 1. Synthesis of tetraazaoctaphyrin **3**.

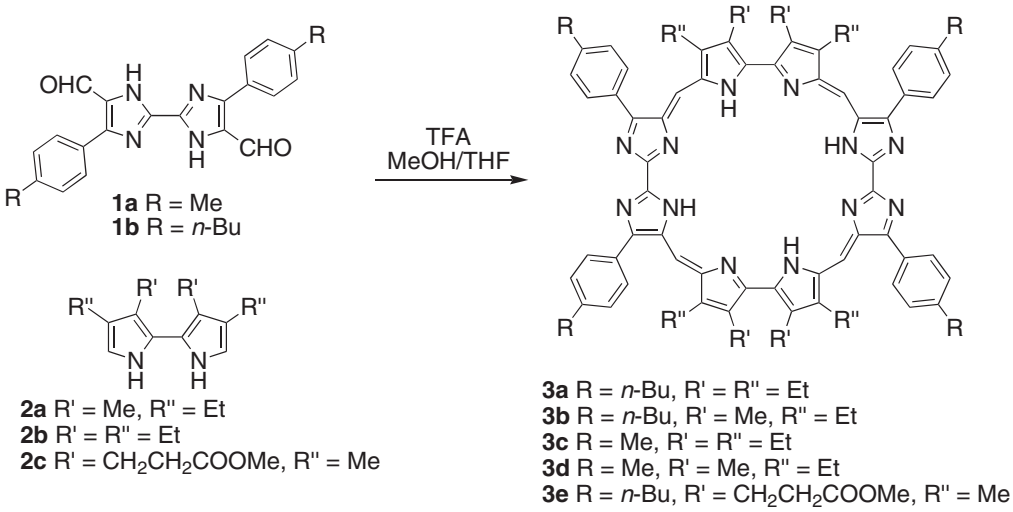

1a R = Me
1b R = *n*-Bu

2a R' = Me, R'' = Et
2b R' = R'' = Et
2c R' = CH_2CH_2COOMe, R'' = Me

3a R = *n*-Bu, R' = R'' = Et
3b R = *n*-Bu, R' = Me, R'' = Et
3c R = Me, R' = R'' = Et
3d R = Me, R' = Me, R'' = Et
3e R = *n*-Bu, R' = CH_2CH_2COOMe, R'' = Me

Fig. 3. ^{1}H NMR spectrum of compound **3b** (500 MHz, CD_2Cl_2, 298 K). Labeling of peaks follows that given in Scheme 2.

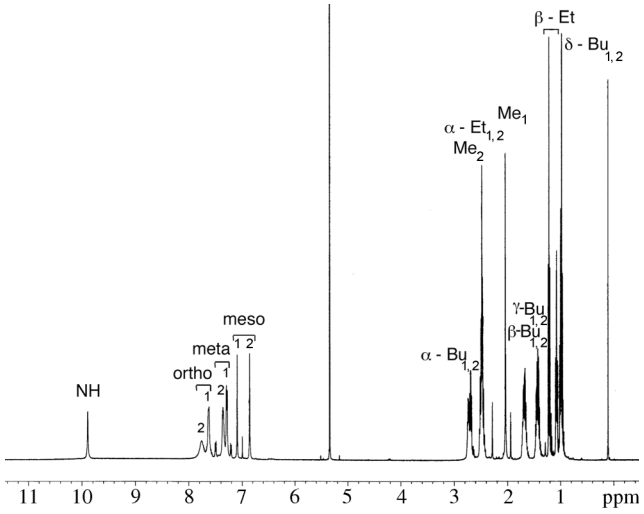

Scheme 2. Labeling scheme used in the analysis of ^{1}H NMR spectra of **3b**. For simplification, π bonding in the macrocycle is not shown. Placement of pyrrole and imidazole NH protons is arbitrary.

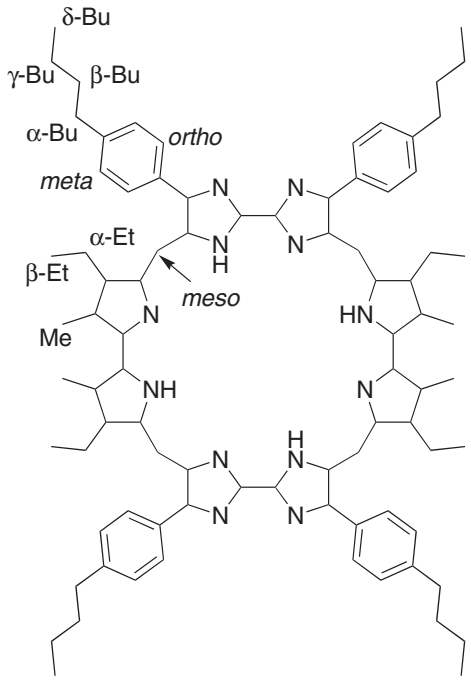

nonequivalent subunits 1 and 2 (Scheme 3). Each of the subunits contains one pyrrole ring and one imidazole ring linked by a meso-bridging carbon atom. In addition, four special ROE correlations provided the information necessary to determine the arrangement of constituent rings in each subunit. The meso signal of subunit 1 ($meso_1$, 7.04 ppm) correlates with the ortho signal of the adjacent aryl ring ($ortho_1$, 7.59 ppm, peak A in Fig. 5), as well as with one of the ethyl CH_3 signals (β-Et1, 1.04 ppm, peak C). In the other subunit, the meso signal ($meso_2$, 6.95 ppm) only correlates with the respective ethyl group (β-Et2, 1.21 ppm, peak D) and shows no cross-peak to the ortho signal ($ortho_2$, 7.72 ppm). However, the latter yields an unexpected correlation with the pyrrolic NH (peak B). This latter correlation can be rationalized by assuming a "kinked" conformation for subunit 2, in which the meso CH fragment is turned away from the aryl ring (Scheme 3).

Macrocycle **3** should contain two subunits of type 1 and two of type 2 combined in such a way that the entire structure exhibits twofold symmetry. The four arrangements that meet the above criterion are shown in Fig. 6. In arrangements A and B, the sequence of subunits in the ring is 1–2–1–2, whereas, in arrangements C and D, the sequence is 1–1–2–2. Furthermore, the aryl rings pointing towards the inside of the macrocycle are positioned on the same side of the macrocyclic plane (in arrangements A and C) or on the opposite sides (B and D). As a result, we obtain four distinct conformers, two of which are chiral (A and D).

Inspection of the molecular models leads to the inference that arrangement B is the least congested of the four conformers and hence the one with the lowest energy. This conclusion is supported by DFT calculations performed at the TZ2p atomic level. Optimized geometries and relative

Fig. 4. ^{1}H COSY spectrum of **3b** (500 MHz, CD_2Cl_2, 298 K). Parts (*A*) and (*B*) show expansions of the aromatic and aliphatic regions, respectively. Peaks corresponding to the symmetrical form are not labeled.

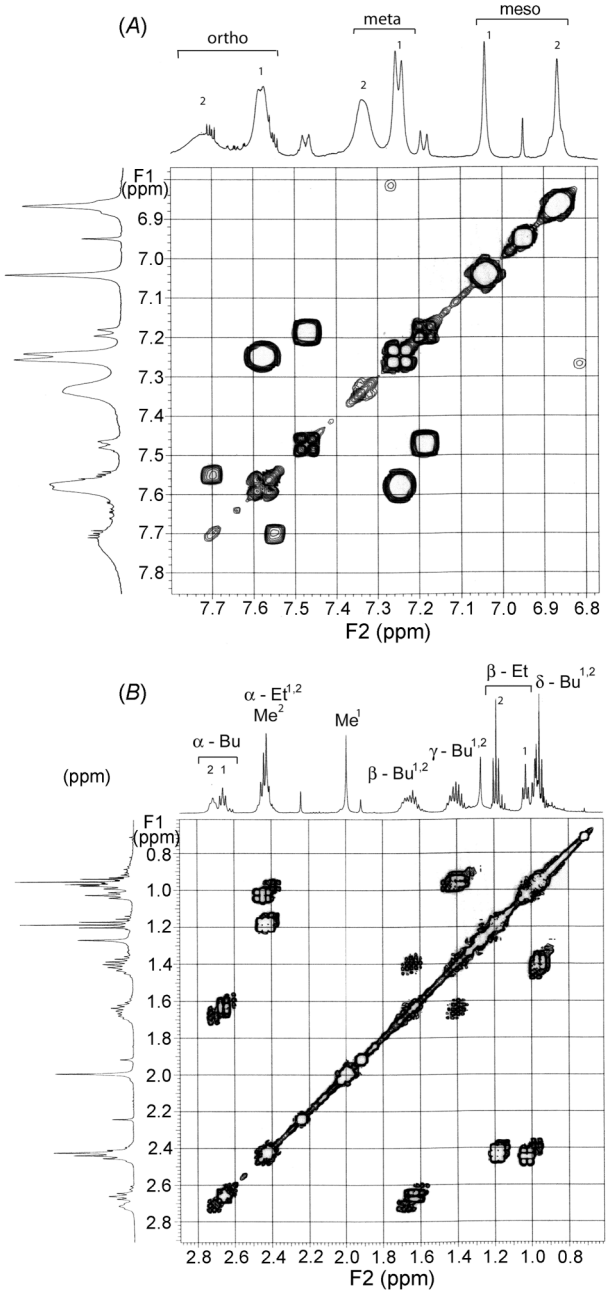

Fig. 5. ^{1}H ROESY spectrum of **3b** (500 MHz, CD_2Cl_2, 298 K). Parts (*A*) and (*B*) show the expansions of aromatic–aromatic and aliphatic–aromatic regions, respectively. The spectrum is phased to give positive ROE crosspeaks.

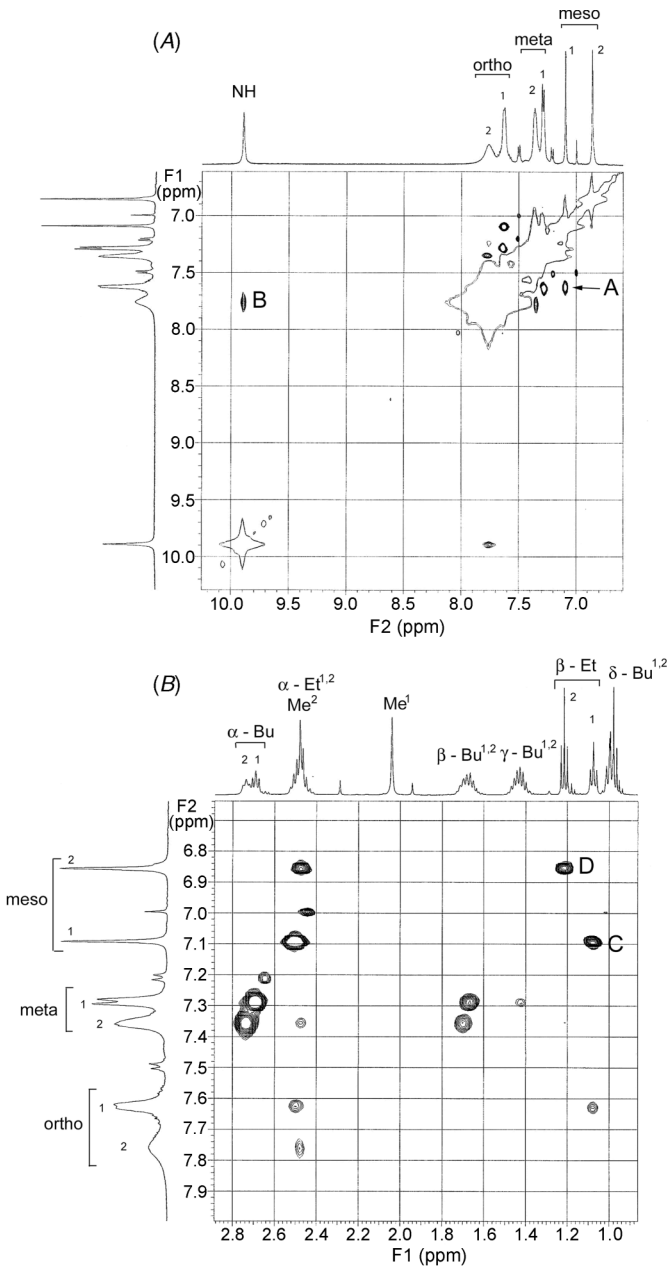

energy values are given in Table 1. Conformer B is the most stable, closely followed in energy by conformer D (Fig. 6); not surprisingly, conformations A and C are higher in energy, likely reflecting the cis arrangement of the phenyl rings within the cavity. Additionally, conformer C, expected to have a symmetry plane (C_s symmetry), collapsed upon optimization into a completely nonsymmetrical geometry.

The conformation of **3** observed in solution appears to be rigid. No exchange cross-peaks in the room temperature ROESY and NOESY spectra have been observed between topologically equivalent signals (e.g., meso$_1$ and meso$_2$); nor has any exchange been noted between the major asymmetrical form and the symmetrical admixture mentioned earlier. In point of fact, the lines remain sharp even at 130 °C in DSMO-d_6. However, significant broadening is observed at room temperature for the ortho and meta signals of the aryl rings (Fig. 3). This broadening is most readily interpreted in terms of the aryl moieties being in an unsymmetrical environment and undergoing slow rotation, conclusions that are consistent with the nonplanar conformation noted above.

Interestingly, the conformation proposed for **3** has no apparent precedent among the structures of octaphyrins

Fig. 6. Possible conformers of tetraazaoctaphyrin **3** (top). The bottom part shows the DFT optimized structures and their point symmetries. Within the optimized structures, subunit 1 is highlighted in blue, while subunit 2 is highlighted in red for clarity. With the exception of the NH hydrogen atoms, all the hydrogen atoms have been removed for clarity.

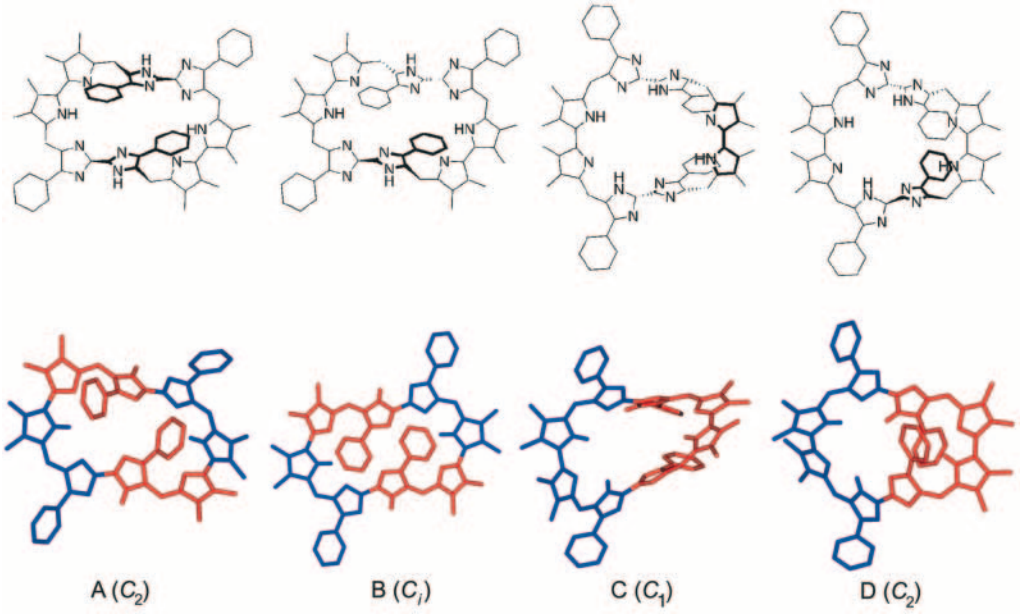

Scheme 3. Illustration of the two subunit structure of **3b**, as determined from the interpretation of the ROESY spectrum. The π electron extended conjugation is removed for clarity.

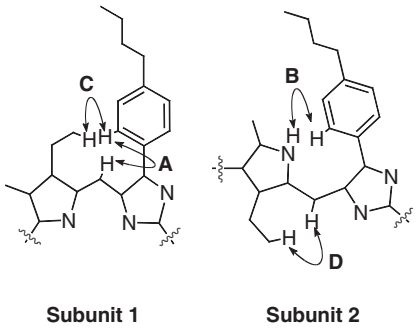

reported to date. For [32]octaphyrin(1.0.1.0.1.0.1.0), reported by Vogel and co-workers (18), a D_2-symmetrical figure eight conformation with transoid bipyrrole subunits located at the figure eight intersection was observed in the crystal structure. A similar conformation was conjectured for a closely related macrocycle obtained by Setsune et al. (19). Another type of figure eight conformation was observed for [36]octaphyrin(1.1.1.1.1.1.1.1), reported by Furuta, Osuka and co-workers. (20), and for its thiophene analogue obtained by Spruta and Latos-Grażyński (21). However, the presence of four imidazole rings in system **3** and a different substitution pattern (aryl groups at the β-pyrrole positions) may explain why this new macrocycle adopts a conformation different from that of its all-pyrrole analogue (18).

Conclusion

The design and synthesis of a novel expanded porphyrin has been described. The series of tetraazaoctaphyrins **3a**–**3e** were formed from the condensation of biimidazole dialdehydes **2a** and **2b** with bis-α-free bipyrroles **2a**–**2c**. The high density of NH functionality makes these systems of potential interest as anion receptors. Initial qualitative tests of this postulate have been performed on tetraazaoctaphyrin **3**. We have found that the neutral host (**3b**) undergoes a naked-eye detectable color change in the presence of fluoride, bromide

Table 1. Minimization energy values for molecular arrangements A–D.

Arrangement	Energy (kcal/mol)	Relative energy
A	–321 084.01	16.76
B	–321 067.25	0
C	–321 053.80	13.45
D	–321 064.63	2.62

Note: 1 cal = 4.184 J.

Fig. 7. Tetraazaoctaphyrin **3b** in acetonitrile in the absence (left) and presence of tetrabutylammonium chloride (middle) and tetrabutylammonium bromide (right).

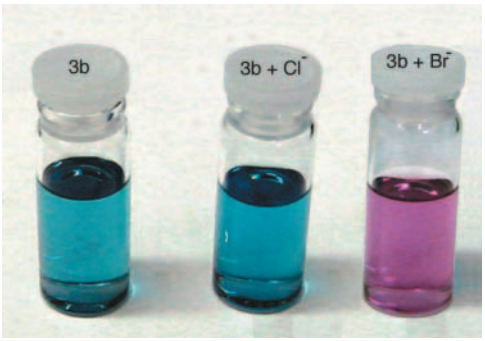

(Fig. 7), cyanide, hydroxyde, acetate, nitrate, dihydrogenphosphate anions (studied in the form of their respective tetrabutylammonium salts). On the other hand, no change in the spectral properties of **3b** was noted upon addition of chloride, iodide, hypochlorate, nitrite, benzoate, and hydrogensulfate anions. Such observations lead us to propose that this or other neutral biimidazole-incorporated expanded porphyrins may emerge as useful anion sensors.

Experimental

General information

All reagents and solvents were purchased from Sigma-Aldrich Corporation, Fischer Scientific, or Fluka and used without further purification with the following exceptions. Dichloromethane was dried by distillation under argon over calcium hydride. Dimethylformamide was dried by passage through two columns of molecular sieves. Tetrahydrofuran (THF) was dried by passage through two columns of activated alumina. Toluene was dried by passage through two columns of activated alumina. *N*-Bromosuccinimide was recrystallized from boiling water. For column chromatography, silica gel (Scientific Adsorbents Inc., particle size 32–63 μm) was used as the immoble phase.

*1-((2-(Trimethylsilyl)ethoxy)methyl)-2-(1-((2-(trimethylsilyl)ethoxy)methyl)-5-formyl-4-*p*-tolyl-1*H*-imidazol-2-yl)-4-*p*-tolyl-1*H*-imidazole-5-carbaldehyde*

4,4′-Dibromo-1,1′-bis[(trimethylsilyl)ethoxymethyl]-2,2′-biimidazole-5,5′-dicarbaldehyde (10) (1.68 mmol) and *p*-methylphenyl boronic acid (3.36 mmol) were degassed for 20 min in 9.2 mL of 2 mol/L sodium carbonate and 4 mL of ethanol by purging the solution with argon. Palladium tetrakistriphenylphosphine (10% mol) was added and the reaction was heated to reflux for 7 h using an oil bath. The reaction flask was removed from the oil bath, cooled, and the mixture was diluted with ethyl acetate, dried with sodium sulfate, filtered, and concentrated in vacuo to give an oil. Column chromatography was performed using silica gel as the solid support, eluting initially with hexanes and slowly increasing the polarity to 20% ethyl acetate in hexanes. Desired fractions were combined, concentrated in vacuo, and dried to give an off-white solid in 89% yield. ^{1}H NMR ($CDCl_3$, 400 MHz) δ: –0.13 (m, 9H), –0.08 (m, 9H), 2.02 (s, 3H), 2.42 (s, 3H), 3.58 (m, 4H), 4.10 (m, 4H), 6.31 (s, 2H), 6.37 (s, 2H), 7.30 (d, J = 8.0 Hz, 4H), 7.61 (d, J = 7.6 Hz, 4H), 9.88 (s, 1H), 9.96 (s, 1H). ^{13}C NMR δ: 14.17, 17.86, 21.35, 60.39, 66.41, 127.14, 127.55, 128.75, 128.95, 129.29, 120.49, 129.525, 139.71, 141.16, 154.49, 171.17, 181.00. HR-MS (CI^+) m/z ($M + H^+$) calcd. for $C_{22}H_{18}N_4O_2$: 371.1508; found: 371.1521.

*2-(5-Formyl-4-*p*-tolyl-1*H*-imidazol-2-yl)-4-*p*-tolyl-1*H*-imidazole-5-carbaldehyde (1a)*

The previous compound (0.457 mmol) was dissolved in 10 mL ethanol. Ten milliliters of 10% HCl was added and the reaction was heated to reflux for 1 h using an oil bath. The flask was removed from the oil bath, cooled, and the solution was carefully neutralized with 10% aqueous sodium carbonate. At this juncture, a solid precipitated out of solution. It was filtered and washed with ice-cold water, and dried under vacuum to give the desired compound in the form of a white solid in 78% yield; mp 160–180 °C. ^{1}H NMR (400 MHz, DMSO-d_6) δ: 2.37 (s, 6H), 7.33 (d, J = 7.6 Hz, 4H), 7.79 (d, J = 8.4 Hz, 4H), 9.88 (s, 2H). ^{13}C NMR (500 MHz, DMSO-d_6) δ: 21.00, 125.30, 126.81, 128.73, 128.97, 129.30, 129.58, 129.72, 133.12, 139.25, 140.01, 182.60. HR-MS (CI^+) m/z ($M + H^+$) calcd. for $C_{22}H_{18}N_4O_2$: 371.1508; found: 371.1521.

General procedure for the preparation of tetraazaoctaphyrin derivatives (3)

Biimidazole dialdehyde **1** (0.184 mmol) was dissolved in 200 mL of dry 2:1 methanol–THF containing 1 mL of TFA. Bipyrrole **2** (0.184 mmol) was separately dissolved in 40 mL of the same solvent ratio and placed in an addition funnel. The bipyrrole solution was added dropwise to the biimidazole solution over 30 min and after several hours of stirring at room temperature, an additional 1 mL of TFA was added to the reaction. Stirring was continued overnight with the reaction left open to the atmosphere. After 12 h, the deep blue-black solution was concentrated in vacuo to give a deep purple oil, which was taken to dryness on the vacuum line to remove any residual trifluoroacetic acid. Column chromatography was performed twice over silica gel, eluting initially with methylene chloride before the polarity of the eluent was slowly increased to 3% methanol in methylene chloride. The desired fractions were combined and concentrated in vacuo to give a lustrous blue-black solid. The material was then redissolved in methylene chloride, washed with 5% aqueous sodium bicarbonate, dried over sodium sulfate, filtered, concentrated in vacuo to a blue-black solid, and dried under vacuum. The solid was triturated with distilled pentane to remove any remaining grease. The desired tetraazaoctaphyrin was obtained as a blue-black lustrous solid.

Elemental analysis was pursued as a means of characterization and repeatedly resulted in carbon, hydrogen, and nitrogren counts of 95%–96% of the theoretical values. XPS analysis revealed the presence of 3.14% silicon in the sample of **2.5b**. Taking into account this silicon percentage, the calculated impurity reveals 1.40 equiv. of the siloxane for each equivalent of the host **2.5b**. Anal. calcd. for $C_{84}H_{92}N_{12}\cdot 1.4SiO_2(CH_3)_2$: C 74.72, H 7.20, N 12.05; found: C 74.71, H 7.09, N 12.22. Efforts to remove the impurity included recrystallization, trituration, and extraction, but unfortunately all proved unsuccesful.

*2,7,20,25-Tetra-*p*-butylphenyl-11,12,15,16,29,30,33,34-octaethyl–3,6,21,24-tetraaza[32]octaphyrin(1.0.1.0.1.0.1.0) (3a)*

The compound was obtained from the condensation of biimidazole **1b** (10) with bipyrrole **2b** (16)[4] in 69% yield, following the general procedure given above. UV–vis (CH_3CN, nm (ε)) λ_{max}: 296 (85 800), 534 (41 100), 631 (94 300). ^{1}H NMR (500 MHz, CD_2Cl_2) δ: 0.95–1.09 (comp, 24H, CH_2CH_3, $CH_2CH_2CH_2CH_3$), 1.13–1.21 (comp, 8H, CH_2CH_3), 1.39–1.49 (comp, 8H, $CH_2CH_2CH_2CH_3$), 1.61–1.75 (comp, 8H, $CH_2CH_2CH_2CH_3$), 2.34 (m, 8H, CH_2CH_3), 2.65–2.77 (comp, 12H, CH_2CH_3 & $CH_2CH_2CH_2CH_3$), 2.97 (m, 4H, $CH_2CH_2CH_2CH_3$), 6.94 (s, 2H, *meso-H*), 7.080 (s, 2H, *meso-H*), 7.27 (d, J = 8.0 Hz, 4H), 7.38 (d, J = 8.5 Hz, 4H), 7.53 (d, J = 8.0 Hz, 4H), 7.82 (d, J = 8.0 Hz, 4H), 9.98

(s, 2H, *NH*), 11.70 (br, *NH*). ^{13}C NMR (500 MHz, CD_2Cl_2) δ: 12.95, 13.095, 13.18, 15.12, 16.33, 17.11, 17.21, 18.19, 21.44, 21.59, 32.26, 32.43, 34.59, 34.64, 117.92, 123.68, 126.87, 127.59, 128.09, 128.45, 134.20, 134.86, 136.08, 137.16, 139.27, 141.34, 144.15, 144.29, 148.18, 150.13, 158.59.

2,7,20,25-Tetra*-p-*butylphenyl-11,16,29,34-tetraethyl-12,15,30,33-tetramethyl-3,6,21,24-tetraaza[32]octaphyrin-(1.0.1.0.1.0.1.0) (3b)

The compound was obtained from the condensation of biimidazole **1b** (10) with bipyrrole **2a** (16)[4] in 54% yield, following the general procedure given above. UV–vis (CH_3CN, nm (ε)) λ_{max}: 299 (139 000), 536 (68 500), 633 (142 000). ^{1}H NMR (500 MHz, CD_2Cl_2) δ: 0.93–1.04 (comp, 18H, CH_2CH_3, $CH_2CH_2CH_2CH_3$), 1.16–1.21 (m, 6H, CH_2CH_3), 1.36–1.47 (m, 8H, $CH_2CH_2CH_2CH_3$), 1.59–1.69 (comp, 8H, $CH_2CH_2CH_2CH_3$), 2.00 (s, 6H, CH_3), 2.39–2.47 (comp, 14H, CH_3 and $CH_2CH_2CH_2CH_3$), 2.61–2.72 (comp, 8H, $CH_2CH_2CH_2CH_3$), 6.87 (br, 2H, *meso-H*), 6.95 (s, 1H, *meso-H*), 7.04 (br, 1H, *meso-H*), 7.19 (m, 2H), 7.25 (m, 2H), 7.46 (br, 4H), 7.49 (m, 2H), 7.59 (br, 2H), 7.72 (br, 4H), 9.87 (br, 2H). ^{13}C NMR (500 MHz, CD_2Cl_2) δ: 10.95, 11.67, 14.11, 14.38, 15.64, 18.16, 18.69, 22.81, 33.98, 35.84, 119.71, 121.37, 126.50, 128.68, 129.10, 129.14, 129.42, 137.88, 143.97, 144.85, 147.48, 159.16.

2,7,20,25-Tetra*-p-*methylphenyl-11,12,15,16,29,30,33,34-octaethyl-3,6,21,24-tetraaza[32]octaphyrin(1.0.1.0.1.0.1.0) (3c)

The compound was obtained from the condensation of biimidazole **1a** with bipyrrole **2b** (16)[4] in 62% yield, following the general procedure given above. UV–vis (CH_3CN, nm (ε)) λ_{max}: 299 (78 400), 540 (40 900), 634 (92 400). ^{1}H NMR (400 MHz, CD_2Cl_2) δ: 0.90–1.25 (comp, 24H, CH_2CH_3), 2.36–2.99 (comp, 28H, CH_3, CH_2CH_3), 6.89 (s, 1H, *meso-H*), 6.99 (s, 2H, *meso-H*), 7.06 (s, 1H, *meso-H*), 7.22–7.31 (comp, 4H), 7.39 (d, J = 7.6 Hz, 2H), 7.54 (m, 4H), 7.72 (d, J = 8.4 Hz, 2H), 7.84 (d, J = 7.6 Hz, 4H), 10.02 (s, 2H). ^{13}C NMR (500 MHz, CD_2Cl_2) δ: 14.81, 15.22, 15.30, 16.86, 18.17, 18.61, 19.18, 19.54, 21.50, 127.81, 128.92, 129.73, 135.12, 138.73, 147.10, 148.25. HR-MS (FAB$^+$) m/z (M + H$^+$) calcd. for $C_{76}H_{77}N_{12}$: 1157.6394; found: 1157.6383.

2,7,20,25-Tetra*-p-*methylphenyl-11,16,29,34-tetraethyl-12,15,30,33-tetramethyl-3,6,21,24-tetraaza[32]octaphyrin-(1.0.1.0.1.0.1.0) (3d)

The compound was obtained from the condensation of biimidazole **1a** with bipyrrole **2a** (16)[4] in 59% yield, following the general procedure given above. UV–vis (CH_3CN, nm (ε)) λ_{max}: 296 (253 000), 531 (140 000), 633 (326 000). ^{1}H NMR (500 MHz, CD_2Cl_2) δ: 1.02 (t, J = 7.5 Hz, 6H), 1.18 (m, 6H), 1.97 (s, 6H), 2.38–2.45 (comp, 6H, CH_3, CH_2CH_3), 6.80 (s, 2H), 7.02 (s, 2H), 7.23 (m, 4H), 7.33 (br, 4H), 7.56 (m, 4H), 7.27 (br, 4H), 9.85 (br, 2H). ^{13}C NMR (500 MHz, CD_2Cl_2) δ: 10.87, 11.55, 14.18, 15.63, 18.17, 18.66, 21.44, 119.89, 121.28, 123.17, 124.99, 126.40, 128.69, 129.44, 129.74, 131.69, 137.54, 138.09, 138.83, 139.80, 147.35, 148.89, 150.94.

2,7,20,25-Tetra*-p-*butylphenyl-11,16,29,34-tetramethyl-12,15,30,33-tetracarboxylate-3,6,21,24-tetraaza[32]octaphyrin(1.0.1.0.1.0.1.0) (3e)

The compound was obtained from the condensation of biimidazole **1b** (10) with bipyrrole **2c** (17) in 26% yield, following the general procedure given above. UV–vis (CH_3CN, nm (ε)) λ_{max}: 275 (34 300), 609 (4790). ^{1}H NMR (400 MHz, CD_2Cl_2) δ: 0.98 (m, 12H, $CH_2CH_2CH_2CH_3$), 1.44 (m, 8H, $CH_2CH_2CH_2CH_3$), 1.67 (m, 8H, $CH_2CH_2CH_2CH_3$), 2.05 (s, 12H, CH_3), 2.45 (t, J = 7.4 Hz, 4H, CH_2CH_2), 2.62–2.77 (comp, 12H, CH_2CH_2), 3.02 (t, J = 7.6 Hz, $CH_2CH_2CH_2CH_3$), 3.21 (t, J = 7.2 Hz, 4H, $CH_2CH_2CH_2CH_3$), 3.30 (s, 6H, CO_2CH_3), 3.56 (s, 6H, CO_2CH_3), 7.00 (s, 2H, *meso-H*), 7.13 (s, 2H, *meso-H*), 7.30 (d, J = 7.6 Hz, 4H), 7.41 (d, J = 8.0 Hz, 4H), 7.62 (d, J = 8 Hz, 4H), 7.82 (d, J = 8 Hz, 4H), 10.02 (s, 2H, *NH*).

Molecular modelling studies

Molecular modelling studies were performed using semi-empirical calculations at the PM3 level, using HyperChem® V7.1, for preoptimization. Density functional theory (DFT) calculations were then performed using PRIRODA-04 (22). A PBE functional that includes the electron density gradient was used. The TZ2p atomic basis sets of grouped Gaussian functions were used to solve the Kohn–Sham equations. The criterion for convergence was to reach a difference in energy gradient between two sequential structures below 0.01 kcal/mol/Å (1 cal = 4.184 J). A PDB file for each optimized structure is included in the Supplementary information.[5]

Acknowledgements

This project was supported by the National Science Foundation Integrative Graduate Education and Research Traineeship Program (grant No. DGE 9870653) and the National Science Foundation (grant No. CHE 0515670 to JLS). We would also like to acknowledge Mr. Jeong Tae Lee for providing bipyrrole **2c** and Dr. Dmitri Laikov for providing the DFT software PRIRODA-04.

References

1. R.B. Woodward. *In* Aromaticity conference. Sheffield, UK. 1966.
2. J.L. Sessler and D. Seidel. Angew. Chem. Int. Ed. **42**, 5134 (2003).
3. J.L. Sessler and S. Weghorn. Expanded, contracted, and isomeric porphyrins. Pergamon, New York. 1997.
4. J.L. Sessler and W.E. Allen. Chemtech, **9**, 16 (1999).
5. J.L. Sessler, M. Cyr, H. Furuta, V. Kral, T. Mody, T. Morishima, M. Shionoyam, and S. Weghorn. Pure Appl. Chem. **3**, 393 (1993).
6. H. Ali and J.E. Van Lier. Chem. Rev. **9**, 2379 (1999).
7. J. Jasat and D. Dolphin. Chem. Rev. **6**, 2267 (1997).

[5] Supplementary data for this article are available on the journal Web site (http://canjchem.nrc.ca) or may be purchased from the Depository of Unpublished Data, Document Delivery, CISTI, National Research Council Canada, Ottawa, ON K1A 0R6, Canada. DUD 5038. For more information on obtaining material refer to http://cisti-icist.nrc-cnrc.gc.ca/irm/unpub_e.shtml.

8. W.J. Youngs, R.S. Simmons, J.C. Garrisoon, W.G. Kofron, and C.A. Tessier. Tetrahedron Lett. **43**, 3423 (2002).
9. A.L. Sargant, I.C. Hawkins, W.E. Allen, H. Liu, J.L. Sessler, and C.J. Fowler. Chem. Eur. J. **9**, 3065 (2003).
10. S. Nonell, J.I. Borrell, S. Borros, C. Colominas, O. Rey, N. Rubio, D. Sanchez-Garcia, and J. Teixido. Chem. Eur. J. **9**, 1635 (2003).
11. J.P. Street. Tetrahedron Lett. **28**, 3333 (1991).
12. Y.D. Choi and J.P. Street. J. Org. Chem. **57**, 1258 (1992).
13. K. Chellappan, N.J. Singh, I. Hwang, J.W. Lee, and K.S. Kim. Angew. Chem. Int. Ed. **44**, 2899 (2005).
14. J. Yoon, S.K. Kim, N.J. Singh, J.W. Lee, Y.J. Yang, K. Chellappan, and K.S. Kim. J. Org. Chem. **69**, 581 (2004).
15. J.L. Sessler and M.C. Hoehner. Synlett, **3**, 211 (1994).
16. M. Ringuet and J. Gagnon. Can. J. Chem. **63**, 2420 (1985).
17. K.M. Kadish, K.M. Smith, and R. Guilard. *In* The porphyrin handbook. Vol. 16. Academic Press, San Diego. 2003.
18. M. Bröring, J. Jendrny, L. Zander, H. Schmickler, J. Lex, Y-D. Wu, M. Nendel, J.G. Cheng, D.A. Plattner, K.N. Houk, and E. Vogel. Angew. Chem. Int. Ed. Engl. **34**, 2511 (1995).
19. J. Setsune, Y. Katakami, and N. Iizuna. J. Am. Chem. Soc. **121**, 8957 (1999).
20. Y-J. Shin, H. Furuta, K. Yoza, S. Igarashi, and A. Osuka. J. Am. Chem. Soc. **123**, 7190 (2001).
21. N. Sprutta and L. Latos-Grażyński. Chem. Eur. J. **7**, 5099 (2001).
22. D.N. Laikov. Chem. Phys. Lett. **281**, 151 (1997).